文章编号： 1007-8827(2015)05-0397-07

碳纳米管/聚酰胺纳米复合材料的制备及其阻燃和热性能

Meisam Shabanian[1], Mohsen Hajibeygi[2], Mehdi Roohani[1]

(1. *Faculty of Chemistry and Petrochemical Engineering*, *Standard Research Institute* (*SRI*), *Karaj P. O. Box* 31745-139, *Iran*;
2. *Faculty of Chemistry*, *Kharazmi University* 15719-14911 *Tehran*, *Iran*)

摘 要： 首先通过壬二酸和双(对-羧苯基)苯基氧化膦直接缩聚反应得到半芳香聚酰胺(PA),采用溶液共混方法,以多壁碳纳米管(CNTs)增强 PA 得到新型纳米复合材料。通过 TG-DSC 和微尺度燃烧量热法探讨 CNTs 对复合材料的热性能和可燃性能的影响。当 CNT 添加量为 5% 时复合材料的失重率比纯 PA 提高 5%,热分解温度提高 70 ℃。与纯 PA 相比,复合材料的热释放速率降低,这表明 CNTs 能提高 PA 的阻燃性。

关键词： 多壁碳纳米管;纳米复合材料;聚酰胺;阻燃

中图分类号： TB332 **文献标识码：** A

通讯作者：Meisam Shabanian. E-mail：m. shabanian@ standard. ac. ir

Synthesis of a novel CNT/polyamide composite containing phosphine oxide groups and its flame retardancy and thermal properties

Meisam Shabanian[1], Mohsen Hajibeygi[2], Mehdi Roohani[1]

(1. *Faculty of Chemistry and Petrochemical Engineering*, *Standard Research Institute* (*SRI*), *Karaj P. O. Box* 31745-139, *Iran*;
2. *Faculty of Chemistry*, *Kharazmi University* 15719-14911 *Tehran*, *Iran*)

Abstract: A novel composite based on a semi-aromatic polyamide (PA) reinforced by multiwall carbon nanotubes (CNTs) was prepared by a solution mixing method. PA was synthesized through a direct polycondensation between azelaic acid and bis (3-amino phenyl) phenyl phosphine oxide. The effect of the CNT addition on the thermal and flammability properties of the composite were studied by thermogravimetric analysis, differential scanning calorimetry and microscale combustion calorimetry. The temperature at which 5% weight loss occurs is increased by over 70 ℃ by incorporating CNTs into the PA matrix. CNTs improve the flame retardancy of PA, which is manifested by a decrease of the heat release rate and the total heat release of the composite compared with pure PA.

Keywords: Multiwalled carbon nanotube; Nanocomposite; Polyamide; Flame Retardancy.

Received date: 2015-07-03; *Revised date*: 2015-10-10

Corresponding author: Meisam Shabanian. E-mail: m. shabanian@ standard. ac. ir

English edition available online ScienceDirect (http://www. sciencedirect. com/science/journal/18725805).
DOI: 10. 1016/S1872-5805(15)60199-8

1 Introduction

Carbon nanotube (CNT) /polymer nanocomposites have attracted wide scientific and industrial interest owing to their improved or/and imparted varied properties by CNTs. Also, they become increasingly affordable. Three applications of CNT/polymer composites have been discussed recently, including antistatic or conductive materials[1,2], mechanically reinforced materials[3-5] and flame retarded materials[5-8].

Aromatic polyamides are one of the most versatile high-performance materials and display a wide range of applications and properties. Their excellent thermal stability and mechanical properties make them useful for advanced technologies[9,10]. However, applications of aromatic polyamides are often restricted by problems in their fabrication such as poor solubility and high softening or melting temperatures caused by high crystallinity and high stiffness of the polymer backbone, leading to difficult process-ability of resulting polyamides. Many efforts have been made to improve solubility and process-ability of aromatic polyamides by structure modification using aliphatic and aromatic monomers. It is also known that the solubility of polymers is often increased when polar constituents and flexible bonds such as [$-O-$, $-SO_2-$, $-CH_2-$] are incorporated into the polymer backbone owing to the changes of crystallinity and intermolecular interactions[11-18]. Semi-aromatic polyamides are made by a combination of aromatic and aliphatic functional-

ities. They are generally aimed at filling the performance gap between high price polymers such polyaryletherketone and aliphatic nylons. They offer a wide range of properties including transparency, thermal stability, non flammability, good barrier, and solvent resistant properties[19-21]. These polyamides have been reinforced with various fillers[22-24]. Recently, excellent nanocomposites obtained from CNT/polyamide, organoclay/polyamide and metal oxide and hydroxide/ polyamide nanocomposites have been reported[25-27]. Few investigations have been carried out in the thermal properties and flame retardancy of CNT/ semi-aromatic polyamide/ nanocomposites.

Most of the plastic are fabricated from petroleum-based materials. Recently, the productions of bio-based polymers have been a very active research area. Bio-based polymers may be obtained by biotechnology, chemical modification of natural polymers or polymerization of bio-based monomers[28]. Vegetable oils are an attractive and renewable chemicals for polymers owing to their availability, non-toxicity and their biodegradability. Recently, some monomers based on various vegetable oil have been used to synthesis polymeric materials[29-31]. Vegetable oils with acrylic double bonds exhibit high a reactivity for preparation of bio polymeric materials[32]. Oleic acid is a monounsaturated 18-carbon fatty acid mostly found in animal fats and vegetable oils. The oxidation of unsaturated oleic acid in presence of potassium permanganate yields azelaic acid[33] The present study deals with the synthesis of semi-aromatic polyamide (PA) as a matrix of CNT/PA nanocomposites. Different properties of the nanocomposite are presented. Interesting findings on improvement of flame retardancy and thermal properties of the nanocomposites are discussed.

2 Experimental

2.1 Materials

Oleic acid, N-methyl-2-pyrrolidone (NMP), potassium permanganate ($KMnO_4$), pyridine, triphenylphosphine oxide, sulfuric acid, nitric acid, dimethylformamide (DMF), methanol and triphenyl phosphite (TPP) from merck were used without further purification. Commercially available calcium chloride ($CaCl_2$, Aldrich) was dried under vacuum at 150 ℃ for 6 h. CNTs (NC7000, Nanocyl S. A., Sambreville, Belgium) have an average diameter 10 nm, lengths between 5 and 10 μm and a carbon purity of 90%.

2.2 Monomer synthesis

2.2.1 Synthesis of azelaic acid

$KMnO_4$ was used to oxidize the double bond of the oleic acid, forming azelaic acid, according to procedures in the literature[33].

2.2.2 Synthesis of Bis(3-amino phenyl) phenyl phosphine oxide

The diamine containing phosphine oxide was synthesized according to the procedure reported [34]. It was synthesized by a three step reaction from the simple organic compounds such as triphenyl phosphine. At first, triphenyl phosphinewas oxidized to triphenyl phosphine oxide, then it was converted to bis(3-nitrophenyl) phenyl phosphine oxide by concentrated nitric acid in the presence of sulfuric acid. Bis (3-nitrophenyl) phenyl phosphine oxide was reduced to bis(3-aminophenyl) phenyl phosphine oxide with $SnCl_2 \cdot 2H_2O$.

2.3 Synthesis of PA

PA was synthesized by the following steps. 50 mL round-bottom flasks with a stirring bar were filled with 4.0 g bis(3-amino phenyl) phenyl phosphine oxide (14 mmol), 2.7 g azelaic acid (14 mmol), 0.5 g calcium chloride (4.5 mmol), 8.7 mL triphenyl phosphite (28 mmol), 1 mL pyridine and 8 mL N-methyl-2-pyrrolidone (Scheme 1). The reaction mixture was heated under reflux in an oil bath at 60 ℃ for 2 h, 90 ℃ for 2 h, and 120 ℃ for 8 h. Then it was poured into 100 mL of methanol and the precipitated product was collected by filtration and washed thoroughly with hot methanol. Finally, the product was dried at 60 ℃ for 12 h in a vacuum oven until the constant weight (Yield = 95%).

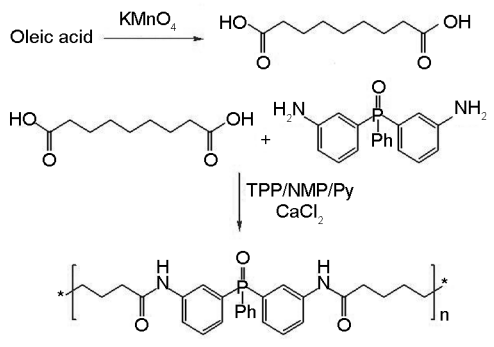

Scheme 1 Synthesis route of PA.

2.4 Preparation of CNT/PA nanocomposite

CNT/PA nanocomposite was prepared by a solution mixing method. 0.02 g CNTs was mixed with 0.98 g PA in N-methyl-2 pyrrolidone (NMP), The mixture was agitated at a high speed at 25 ℃ overnight and ultrasonically irradiated to disperse CNTs uniformly in the PA matrix. By casting the suspension

onto a glass plate and solvent evaporation in a vacuum oven, the final CNT/PA nanocomposite was prepared.

2.5 Characterization

Fourier transform infrared (FT-IR) data were recorded on a Galaxy series FT-IR 5000 spectrophotometer (England). For sample preparation, the powdered species were mixed with KBr and pressed into pellets for further characterization.

^{1}H NMR measurements were performed using a Bruker Avance III 500 spectrometer (Rheinstetten, Germany) operating at 500 MHz (^{1}H). DMSO-d6 was used as the solvent and the solvent signal was used for internal calibration (DMSOd6: δ(^{1}H) = 2.5 ppm).

Determination of weight-average (M_w) and number-average (M_n) molecular weights was performed by size exclusion chromatography (SEC) using an Agilent Series 1100 (Agilent) system equipped with a pump, degasser and differential refractive index (RI) detector. Two Zorbax PSM Trimodal-S 250 mm × 6.2 mm columns (Rockland Tech, USA) were used. The measurements were performed using a mixed eluent N, N-dimethylacetamide (DMAc) with 2 vol% water and 3 g/L LiCl at a flow rate of 0.5 mL/min. The molar mass was calculated after calibration with poly(2-vinylpyridine).

The morphological analysis was carried out using transmission electron microscopy (TEM) on a LEO 912 microscope operated with an acceleration voltage of 120 kV at room temperature in bright field illumination mode. For preparing TEM samples, two approaches were used. In the case of CNT, its ethanol suspension was dropped directly into copper grids. For the CNT/PA nanocomposite, ultrathin sections of each sample with a thickness of about 50 nm were prepared by ultramicrotomy.

The thermal stability of the samples was measured by thermogravimetric analysis (TGA, TA instruments Q 5000) in a temperature range between room temperature and 800 ℃ at a heating rate of 10 ℃/min in nitrogen atmosphere. The thermal properties of samples were measured by differential scanning calorimetry (DSC, TA instrument Q 1000) in a temperature range between −80 and 230 ℃ at a heating rate of 10 ℃/min in nitrogen atmosphere.

Microscale combustion calorimeter (MCC, FTT) was used to investigate flammability of the samples[35].

3 Results and discussion

3.1 PA characterization

PA exhibits a number-average molecular weight (M_n) and a weight-average molecular weight (M_w) of 2.1×10^4 and 5.4×10^4 g/mol, respectively, according to poly(vinyl pyridine) (PVP) standard. The polydispersity index is 2.5. Inherent viscosity (η_{inh}) of PA is 0.71 (dL/g) at a concentration of 0.5 g/dL in DMF at 25 ℃.

Fig. 1 shows FT-IR spectrum of PA. The absorption band at 1 655 cm^{-1} is associated with C═O stretching vibration in the main chain of PA, the absorption band at 3 233 cm^{-1} is contributed by N-H stretching of amide groups, the bands at 3 051 and 2 925 cm^{-1} are related to aromatic and aliphatic C-H bond stretching vibrations, respectively, and the band at 1 165 cm^{-1} is ascribed to P═O stretching vibration in the phosphine oxide moiety in the PA backbone.

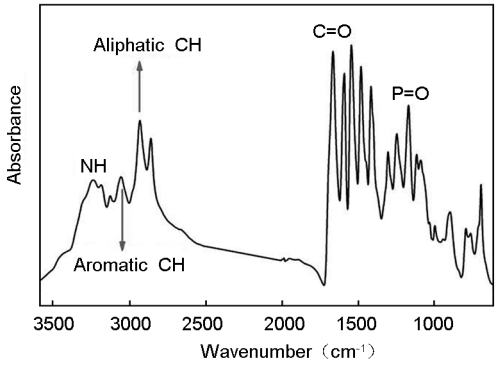

Fig. 1　FT-IR spectrum of PA.

The ^{1}H-NMR spectrum confirms the chemical structure of PA as shown in Fig. 2. The aromatic protons appear in the region of 6.81-7.96 mg/L. The protons related to methylene groups appear in the region of 1.29-2.31 mg/L and the peak in the region of 10.19 mg/L is assigned to N-H amide groups in the PA backbone.

3.2 Characterization of CNT/PA nanocomposite

TEM is utilized as an effective means to have a insight into the internal structure and spatial distribution of the various components, through direct visualization [36]. In general, the drawbacks related to the homogeneous dispersion of the CNTs in the polymer matrix resulted from intrinsic van der Waals attractions between the individual CNT as well as high aspect ratio and large surface area, make it difficult for the CNTs to disperse in the polymer matrix.

The dispersion of CNTs in the polymeric matrix generally depends on the polar interaction between the nanofillers and the polymer matrix. Fig. 3 shows the TEM micrographs of CNT and the CNT/PA nano-

composite. Fig. 3a displays a TEM micrograph of CNTs with an outer diameter of ~10 nm. There are amorphous matters on the CNT surface that can be attributed to dispersion of CNTs in ethanol. Ethanol shows an etching effect on CNTs[37]. From the TEM results, it can be seen that CNTs have been well dispersed within PA matrix with very small aggregations and entanglements of CNTs in the CNT/PA nanocomposite (Fig. 3b). The aggregation of CNTs is attributed to the strong van der Waals interaction between the nanotubes. In the case of the CNT/PA nanocomposite, interaction between CNTs and PA leads to a good dispersion.

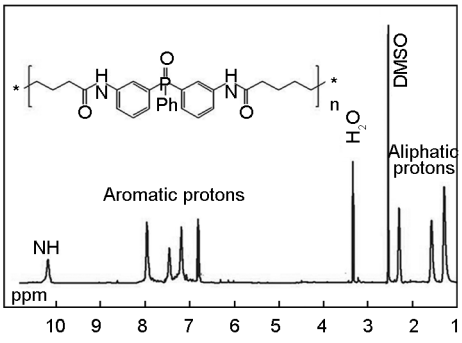

Fig. 2 ^{1}H-NMR spectrum of PA.

The thermal stability and char yields are very important properties in polymeric materials and normally they can be reflected by TGA. The thermal properties of PA and the CNT/PA nanocomposite were investigated by TGA and DSC, which are described in Fig. 4 and summarized in Table 1.

The TGA and DTG of PA show two steps in its thermal decomposition. The main decomposition step occurs between 350 and 500 ℃ with a decomposition peak at around 435 ℃. The char yield of PA is about 26.4%.

This indicates that PA containing long aliphatic chain in its backbone possesses a good thermal stability and a very high char yield as compared with conventional aliphatic polyamides. TGA of CNTs shows a 2.5% weight loss up to 800 ℃. The thermal decomposition behavior of the CNT/PA nanocomposite shows its first decomposition step occurring at much higher temperature than the neat PA with a decomposition peak at 253 ℃. The main decomposition peak is around 426 ℃, similar to PA. It is noticed that CNT/PA nanocomposite has a much higher the 5% weight loss temperature (T_5) and the 10% weight loss temperature (T_{10}) (over 70 ℃) than those of PA, indicating that the introduction of CNTs into PA can significantly improve the thermal stability of PA and delay the decomposition of PA. CNT/PA nanocomposite also has a higher char residue than neat PA at 800 ℃.

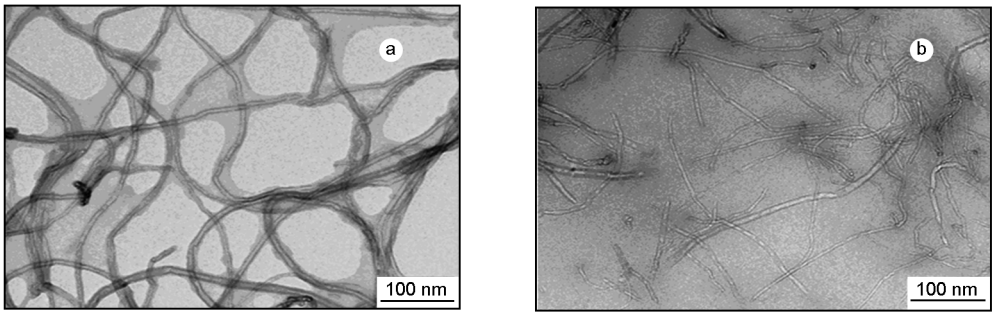

Fig. 3 TEM micrographs of the(a) CNTs and(b) CNT/PA nanocomposite.

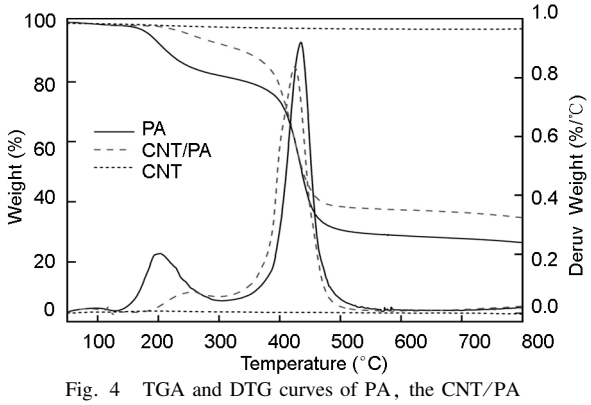

Fig. 4 TGA and DTG curves of PA, the CNT/PA nanocomposite and CNTs.

Differential scanning calorimetry (DSC) was used to determine the glass-transition temperature values (T_g) of the samples. The glass transition temperature (T_g) of PA is at 142 ℃ and that of the CNT/PA nanocomposite is 148 ℃ (Fig. 5). The onset of decomposition temperature of CNT/PA nanocomposite is higher than that of PA. Thus, it means that incorporation of CNTs into PA matrix and interaction between PA chains and CNTs improve the thermal stability and increase T_g values of the nanocomposite.

Table 1　Thermal properties of PA and the CNT/PA nanocomposite.

Samples	T_5(℃)[a]	T_{10}(℃)[a]	T_{50}(℃)[a]	Char yield [b]	T_g[c]
PA	190	215	436	26.4	142
CNT/PA nanocomposite	262	342	438	34.7	148

Note: [a] Temperature at which 5% ,10% and 50% weight loss was recorded by TGA at a heating rate of 10 ℃/min under N_2. [b] Weight percentage of material left after TGA analysis at 800 ℃. [c] Glass transition temperature was recorded at a heating rate of 10 ℃ min^{-1} in a nitrogen atmosphere.

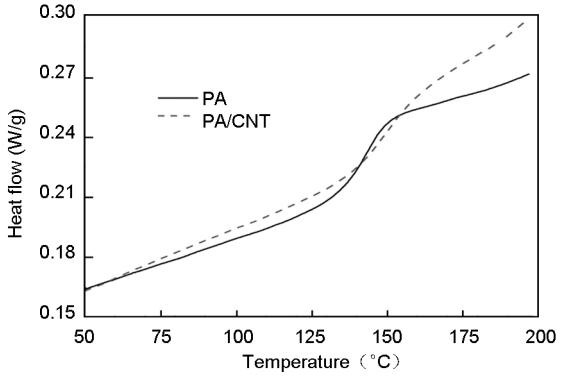

Fig. 5　DSC curves of the PA and CNT/PA nanocomposite.

The microscale combustion calorimeter (MCC) is a fast and convenient technique developed for the investigation of the flammability of polymers. The parameters measured from this test are heat release rate (HRR) and the total heat release (THR). The HRR plots for PA and the CNT/PA nanocomposite are shown in Fig. 6 and the corresponding combustion data is presented in Table 2. It can be found that the values of peak HRR (pHRR) in the CNT/PA nanocomposite are lower than that of PA. The pHRR value of neat PA is 296.3 W/g, and the pHRR of the CNT/PA nanocomposite is 264.3 W/g, indicating that the nanocomposite has a low flammability. The THR calculated from the area under the HRR curve is also an important parameter for fire hazard evaluation. The CNT/PA nanocomposite has a lower THR value of 17.8 kJ · g^{-1} than neat PA (19.7 kJ · g^{-1}). It is noted that the THR values of the CNT/PA nanocomposite is not much lower than PA. This might be relevant to the high heat transfer of CNTs. CNTs may influence the fire behavior of the polymer by changing energy absorption and heat conductivity[38]. The CNT/PA nanocomposite has a higher char residue at high temperatures than neat PA. This could lead to a better flame retardancy of the nanocomposite. Besides the char resides have an impact on the flame retardancy for both of PA and CNT/PA nanocomposite. Another possible flame retardant mechanism for the PA and CNT/PA nanocomposite is that the phosphine oxide moieties in PA backbone might release some phosphorus containing radicals which can capture the H· and HO· in gas phase, so that the flammability of the PA and CNT/PA nanocomposites is lowered. All the above results suggest that the introduction of CNTs could improve flame retardancy of PA.

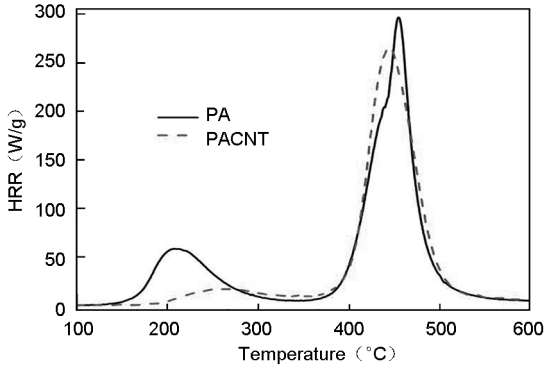

Fig. 6　HRR curves of the PA and CNT/PA nanocomposite.

Table 2　MCC measurement data

Samples	pHRR (W/g)[a]	THR (kJ/g)[b]
PA	296.3	19.7
CNT/PA nanocomposite	264.3	17.8

Note: [a] Peak heat release rate; [b] The total heat release.

4　Conclusions

A novel bio-based semi-aromatic CNT reinforced PA nanocomposite was fabricated by a solution mixing method. PA was synthesized through polycondensation between the phosphorus diamine and bio-based azelaic acid. The introduction of phosphine oxide and aliphatic groups enhances solubility and improves glass transition temperature of PA. CNTs have a good dispersion in PA matrix. Study on the thermal degradation of the CNT/PA nanocomposite reveals that the introduction of CNTs into PA matrix can significantly increase the thermal stability of PA. The CNT/PA nanocomposite has also an increased char yield. The presence of CNTs in PA matrix improves the flame retardancy of PA by decreasing pHRR and THR values.

References

[1] Song W L, Wang W, L Monica Veca, et al. Polymer/carbon nanocomposites for enhanced thermal transport properties-Carbon nanotubes versus graphene sheets as nanoscale fillers[J]. Journal of Materials Chemistry, 2012, 22(33): 17133-17139.

[2] Al-Saleh M H, U Sundararaj. Microstructure, electrical, and electromagnetic interference shielding properties of carbon nanotube/acrylonitrile-butadiene-styrene nanocomposites[J]. Journal of Polymer Science, Part B: Polymer Physics, 2012, 50(19): 1356-1362.

[3] Ghasemi I, A T Farsheh, Z Masoomi. Effects of multi-walled carbon nanotube functionalization on the morphological and mechanical properties of nanocomposite foams based on poly(vinyl chloride)/(wood flour)/(multi-walled carbon nanotubes)[J]. Journal of Vinyl and Additive Technology, 2012, 18(3): 161-167.

[4] Díez-Pascual A M, Mohammed N, Carlos M, et al. High-performance nanocomposites based on polyetherketones[J]. Progress in Materials Science, 2012, 57(7): 1106-1190.

[5] Ma P C, Siddiqui Naveed A, Gad Marom, et al. Dispersion and functionalization of carbon nanotubes for polymer-based nanocomposites: A review[J]. Composites Part A: Applied Science and Manufacturing, 2010, 41(10): 1345-1367.

[6] Shabanian M, Nian-Jun Kang, De-Yi Wang, et al. Synthesis, characterization and properties of novel aliphatic-aromatic polyamide/functional carbon nanotube nanocomposites via in situ polymerization[J]. RSC Advances, 2013, 3(43): 20738-20745.

[7] Hapuarachchi T D , T Peijs. Multiwalled carbon nanotubes and sepiolite nanoclays as flame retardants for polylactide and its natural fibre reinforced composites[J]. Composites Part A: Applied Science and Manufacturing, 2010, 41(8): 954-963.

[8] Abbaszadeh S, Allec N, Karim K S. Characterization of low dark-current lateral amorphous-selenium metal-semiconductor-metal photodetector[J]. IEEE Electron Device Letters, 2011, 32(9): 1263-1265.

[9] Cassidy P E. Thermally stable polymers: syntheses and properties[M]. 1980, Marcel Dekker Inc.

[10] García J M, Félix C, García, Felipe Serna, et al. High-performance aromatic polyamides[J]. Progress in Polymer Science, 2010, 35(5): 623-686.

[11] Mallakpour S, M Kolahdoozan. Synthesis and properties of novel soluble aromatic polyamides derived from 5-(2-phthalimidyl-3-methyl butanoylamino) isophthalic acid and aromatic diamines[J]. Reactive and Functional Polymers, 2008, 68(1): 91-96.

[12] Bazzar M, M Ghaemy, R Alizadeh. Novel fluorescent light-emitting polymer composites bearing 1,2,4-triazole and quinoxaline moieties: Reinforcement and thermal stabilization with silicon carbide nanoparticles by epoxide functionalization[J]. Polymer Degradation and Stability, 2012, 97(9): 1690-1703.

[13] Song R, D Yang, L He. Preparation of semi-aromatic polyamide(PA)/multi-wall carbon nanotube (MWCNT) composites and its dynamic mechanical properties[J]. Journal of Materials Science, 2008, 43(4): 1205-1213.

[14] Shabanian M, M Hajibeygi. Magnetic heat resistant poly(amide-imide) nanocomposite derived from bisphenol A: Synthesis and properties[J]. Polymer Composites, 2013, 34(10): 1682-1689.

[15] Faghihi K, M Hajibeygi, M Shabanian. Novel thermally stable poly(amide-imide)s containing dibenzalacetone moiety in the main chain: Synthesis and characterization[J]. Macromolecular Research, 2010, 18(5): 421-428.

[16] Faghihi K, Shabanian M, Hajibeygi M , et al. Synthesis and characterization of new poly(ether-ester-imide)s as a generation of soluble and thermally stable polymers[J]. Polymer Bulletin, 2010, 66(1): 37-49.

[17] Shabanian M, D Ghanbari. Synthesis of magnesium hydroxide nanofiller and its use for improving thermal properties of new poly(ether-amide)[J]. Journal of Applied Polymer Science, 2013, 127(3): 2004-2009.

[18] Shabbir S, et al. Synthesis, characterization and functionalization of thermally stable hyperbranched polyamide-ethers based on 6-hydroxy-2,4-bis(4′-nitrobenzamide)pyrimidine[J]. Polymer Degradation and Stability, 2010, 95(4): 500-507.

[19] Shabanian M, Nian-Jun Kang, De-Yi Wang, et al. Synthesis of aromatic-aliphatic polyamide acting as adjuvant in polylactic acid (PLA)/ammonium polyphosphate (APP) system[J]. Polymer Degradation and Stability, 2013, 98(5): 1036-1042.

[20] Zulfiqar S, M Ishaq, M Ilyas Sarwar. Synthesis and characterization of soluble aromatic-aliphatic polyamide[J]. Advances in Polymer Technology, 2010, 29(4): 300-308.

[21] Zulfiqar S, Zahoor Ahmad, Muhammad Ishaq, et al. Aromatic-aliphatic polyamide/montmorillonite clay nanocomposite materials: Synthesis, nanostructure and properties[J]. Materials Science and Engineering: A, 2009, 525(1-2): 30-36.

[22] Sarwar M I, S Zulfiqar, Z Ahmad. Properties of polyamide-zirconia nanocomposites prepared from sol-gel technique[J]. Polymer Composites, 2009, 30(1): 95-100.

[23] Zulfiqar S, Ayesha K, Muhammad R, et al. Probing the role of surface treated montmorillonite on the properties of semi-aromatic polyamide/clay nanocomposites[J]. Applied Surface Science, 2008, 255(5): 2080-2086.

[24] Shabanian M, Basaki N. New photosensitive semi aramid/organoclay nanocomposite containing cinnamoyl groups: Synthesis and characterization[J]. Composites Part B: Engineering, 2013, 52: 224-232.

[25] Zulfiqar, S, Ishaq M, Sarwar M I. Effect of surface modification of montmorillonite on the properties of aromatic polyamide/clay nanocomposites[J]. Surface and Interface Analysis, 2008, 40(8): 1195-1201.

[26] Zhao H, et al. Improving the performance of polyamide reverse osmosis membrane by incorporation of modified multi-walled carbon nanotubes[J]. Journal of Membrane Science, 2014. 450(0): 249-256.

[27] Mallakpour S, Hatami M. Production and evaluation of the surface properties of chiral poly(amide-imide)/TiO_2 nanocomposites containing L-phenylalanine units[J]. Progress in Organic Coatings, 2012,74(3): 564-571.

[28] Pardal F, Slim Salhi, Brigitte Rousseau, et al. Unsaturated polyamides from bio-Based z-octadec-9-enedioic acid[J]. Macromolecular Chemistry and Physics, 2008, 209(1): 64-74.

[29] Galià M, Lucas Montero de Espinosa, Joan Carles Ronda,? et al. Vegetable oil-based thermosetting polymers[J]. European Journal of Lipid Science and Technology, 2010, 112(1): 87-96.

[30] Zuo J, Shaojun Li, Laziz Bouzidi, et al. Thermoplastic polyester amides derived from oleic acid[J]. Polymer, 2011, 52(20): 4503-4516.

[31] Roumanet P J, Lafleche F, Jarroux N, et al. Novel aliphatic polyesters from an oleic acid based monomer. Synthesis, epoxidation, cross-linking and biodegradation[J]. European Polymer Journal, 2013, 49(4): 813-822.

[32] Xia Y, R C Larock. Vegetable oil-based polymeric materials: synthesis, properties, and applications[J]. Green Chemistry, 2010, 12(11): 1893-1909.

[33] McEwen, J H a W. Azelaic acid[J]. Organic Synthese, 1943,

2: 53-54.
[34] Faghihi K, Zamani K. Synthesis and properties of novel flame-retardant poly(amide-imide)s containing phosphine oxide moieties in main chain by microwave irradiation[J]. Journal of Applied Polymer Science, 2006, 101(6): 4263-4269.
[35] Shi Y, Takashi Kashiwag, Richard N Walters, et al. Ethylene vinyl acetate/layered silicate nanocomposites prepared by a surfactant-free method: Enhanced flame retardant and mechanical properties[J]. Polymer, 2009, 50(15): 3478-3487.
[36] Kiliaris P, Papaspyrides C D. Polymer/layered silicate (clay) nanocomposites: An overview of flame retardancy[J]. Progress in Polymer Science, 2010, 35(7): 902-958.
[37] Yu G, Gong J L, Wang S, et al. Etching effects of ethanol on multi-walled carbon nanotubes[J]. Carbon, 2006, 44(7): 1218-1224.
[38] Kashiwagi T, Grulke Eric A, Jenny Hilding, et al. Thermal and flammability properties of polypropylene/carbon nanotube nanocomposites[J]. Polymer, 2004, 45(12): 4227-4239.

《新型炭材料》2013 年 ~ 2014 年优秀论文评选结果揭晓

经《新型炭材料》编辑、顾问委员会全体成员无记名投票,按得票多少选出《新型炭材料》2013 年 ~ 2014 年优秀论文如下:

2013 年

No	姓 名	所在单位	文 章 标 题	期:页码
1	侯翠岭等	西北工业大学	碳纳米管/四氧化三铁复合材料的电磁波吸收性能	3: 184-190
2	柯义虎等	陕西师范大学	用废弃印刷线路板非金属组分分离物制备多孔炭	2: 108-114
3	郑冬芳等	北京化工大学	高性能超级电容器用高比表面积、层次孔结构炭材料的简便制备	2: 151-155
4	丁　翔等	清华大学	氧化铜/石墨烯的制备及其电化学性能	3: 172-177
5	张丽芳等	天津大学	石墨烯基宏观体:制备、性质及潜在应用	3: 161-171

2014 年

No	姓 名	所在单位	文 章 标 题	期:页码
1	张　强等	清华大学	碳质材料在锂硫电池中的应用研究进展	4: 241-264
2	徐　超等	福州大学	选择性还原氧化石墨烯	1: 61-66
3	邓洪贵等	华东理工大学	用于锂离子电池的 Fe_3O_4/C 纳米结构的可控制备	4: 301-308
4	王旭珍等	大连理工大学	3D 二硫化钼/石墨烯组装体的制备及其催化脱硫性能	2: 81-88
5	骆文彬等	中国科学院金属研究所	碳纳米管复合磷酸铁锂材料的制备及性能	4: 287-294

《新型炭材料》编辑部

2015 年 10 月